energies

MDPI

Article

Estimating the Impact of Electric Vehicle Demand Response Programs in a Grid with Varying Levels of Renewable Energy Sources: Time-of-Use Tariff versus Smart Charging

Wooyoung Jeon [1], Sangmin Cho [2] and Seungmoon Lee [2,*]

[1] Department of Economics, Chonnam National University, Gwangju 61186, Korea; wyjeon@jnu.ac.kr
[2] Korea Energy Economics Institute, Ulsan 44543, Korea; smin0621@keei.re.kr
* Correspondence: paragon@keei.re.kr; Tel.: +82-52-714-2223

Received: 21 July 2020; Accepted: 19 August 2020; Published: 24 August 2020

check for updates

Abstract: An increase in variable renewable energy sources and soaring electricity demand at peak hours undermines the efficiency and reliability of the power supply. Conventional supply-side solutions, such as additional gas turbine plants and energy storage systems, can help mitigate these problems; however, they are not cost-effective. This study highlights the potential value of electric vehicle demand response programs by analyzing three separate scenarios: electric vehicle charging based on a time-of-use tariff, smart charging controlled by an aggregator through virtual power plant networks, and smart control with vehicle-to-grid capability. The three programs are analyzed based on the stochastic form of a power system optimization model under two hypothetical power system environments in Jeju Island, Korea: one with a low share of variable renewable energy in 2019 and the other with a high share in 2030. The results show that the cost saving realized by the electric vehicle demand response program is higher in 2030 and a smart control with vehicle-to-grid capability provides the largest cost saving. When the costs of implementing an electric vehicle demand response are considered, the difference in cost saving between the scenarios is reduced; however, the benefits are still large enough to attract customers to participate.

Keywords: electric vehicle; demand response; variable renewable sources; time-of-use; smart charging; virtual power plant

1. Introduction

1.1. Background and Motivation

In 2017, the South Korean government implemented an energy transition policy to convert traditional fossil-fuel-oriented energy into eco-friendly renewable energy as a solution to high domestic and international pressure for greenhouse gas emission reduction. The goal of the energy transition policy is to displace coal and nuclear power generation quickly with variable renewable sources (VRS) such as wind and solar energy, which are free from greenhouse gas and fine dust emissions. The plan is to increase the share of renewable sources for power generation in South Korea from 6.2% in 2017 to 20% in 2030 and 30–35% by 2040 [1,2].

The replacement of traditional power sources with VRS can help to build a more eco-friendly and less fossil-fuel-dependent power supply environment; however, VRS can undermine the reliability of the power supply. Unlike coal and nuclear power, VRS sources, such as solar photovoltaic (PV) and wind, cannot produce the required energy in periods of high demand, and the forecasting error for day-ahead dispatch planning is substantially higher. Combined with other uncertainty factors such as variable demand and transmission line failure, this can cause reliability problems in the power supply network.

VRS cause problems in the power system mainly through two characteristics, which are variability and uncertainty. Solar PV typically has high variability issue due to concentrated generation during day time so it requires many fast ramping units to meet the rapid net load changes [3]. Wind power commonly has high uncertainty issue due to difficulty in accurate forecasting so this needs the power system to secure more reserve resources to meet net load deviation from the forecasted value [4].

To successfully implement the transition to a VRS-oriented power system, it is essential to secure enough flexible resources to support a power system undermined by the high variability and uncertainty inherent in VRS. Among various potential flexible resources, energy storage systems (ESS), such as pumped storage or lithium-ion batteries, are considered the most effective. ESS are an effective flexible resource for mitigating the duck curve phenomenon, in which the net load decreases during intense sunlight hours from 11 am to 5 pm due to concentrated PV generation, causing high inefficiency and reliability issues in the power system. ESS can reduce the effect of the duck curve by storing solar power during high generation times and discharging it when required. ESS can also be used as an effective reserve resource to complement the uncertainty of VRS. However, the most commonly used ESS, lithium-ion batteries, are not yet economically feasible as a dedicated resource for power systems, and it is difficult to build additional pumped storage due to geographical conditions and environmental issues.

Demand response (DR) resources, especially electric vehicle (EV) DR resources, are drawing attention as an alternative to ESS. The number of EVs in Jeju Island, Korea, is expected to grow from 23,000 in 2019 to 377,000 in 2030 [5]. The high growth in the number of EVs creates an opportunity to significantly mitigate the variability of a VRS-based power supply if electricity demand from EVs can be shifted to duck curve hours, based on dynamic pricing mechanisms such as a time-of-use (TOU) rate or real-time pricing (RTP).

Moreover, the benefits from the EV DR can be enhanced when virtual power plant (VPP) technology is combined to enable an aggregator to remotely control the charging and discharging of energy when EVs are connected to the power system. Using VPP technology, small batteries in individual EVs can be integrated to function like a large ESS, optimally controlled by an aggregator under the direction of the system operator. An integrated ESS provided by EVs via a VPP network can be economically viable as the cost of the EV battery is now compensated by both operating an EV and by supporting the power system.

1.2. Related Works

Various studies, including References [6–8], discuss the potential benefits of EVs based on smart charging. Reference [6] estimated the benefits of EVs and thermal storage under a flat rate structure and an optimum rate structure which reflects cost saving in generation, reserve, and capacity. Reference [7] analyzed the potential financial return of EVs in a power system demand resources with vehicle-to-grid (V2G) capability when its dual-use service is correctly estimated, namely frequency regulation and peak load reduction. The authors demonstrated that V2G has economic potential for frequency regulation alone; however, when adopted as a dual-use service, the economic benefit is substantially higher. Zhang et al. [8] proposed regime-switching risk management based on vehicle-to-building power sources using EV resources. The authors proposed a two-regime structure: a low-risk regime, whereby the system objective is to minimize charging costs, and a high-risk regime, whereby the intention is to reduce high energy costs due to peak pricing. The results showed that regime-switching management is effective in reducing the cost of energy.

Several studies discuss the impact of EV demand under dynamic pricing mechanisms. Reference [9] evaluated the cost of the new infrastructure required to implement TOU and real-time pricing programs to determine the benefits from policies for shifting EV charging from on-peak to off-peak hours. Reference [10] analyzed EV electricity tariffs based on three aspects: customer acceptance, the potential for load flexibility, and aggregator profitability. The authors concluded that a tariff should be suitable for customers to provide load flexibility and provide adequate benefits to aggregators as well.

In addition, literature such as References [11–13] discusses the high potential of EV as demand resource in the microgrid environment. Reference [11] proposes the two-level microgrid problems such that charging strategy to minimize the charging cost and its impact on the power generation planning of small island grid. Reference [12] discusses two-stage smart charging algorithm in the building equipped with EVs, solar panels and heat pump, and showed V2G is cost-effective under optimal management despite of high degradation cost of EV battery. Reference [13] uses a metaheuristic-based vector-decoupled algorithm to optimally operate microgrid with EVs and stochastic renewable energy sources and showed the EV can provide meaningful services regarding voltage and frequency stabilization in a microgrid.

1.3. Objectives of This Study

In this study, we analyze how effectively EV DR programs can reduce the operating cost and improve the reliability of the power supply system in Jeju Island, where rapid increase in VRS as well as EVs is expected. This study contributes to the literature in three distinct ways as follows.

First, this study analyzes and compares the impact of three EV demand control methods: demand control under a TOU rate, smart charging control by an aggregator using VPP technology with grid-to-vehicle (G2V) capability (hereafter referred to as VPP1), and VPP1 with V2G capability (hereafter referred to as VPP2), which allows not only optimal charging but also discharging to the grid. The TOU program can be considered a passive application of EV DR, while VPP1 is a moderately active application and VPP2 a highly active application. The value of an EV DR program is estimated according to these three application methods.

Second, the cost saving in an EV DR program is separately estimated in a power system with low levels of VRS in 2019 and high levels of VRS in 2030. This separate analysis allows us to compare the benefits from EV DR under variability and uncertainty caused by VRS.

Third, monthly cost saving per EV customer is estimated by varying the participation rate in the DR program. In addition, costs induced to implement the DR program, such as aggregator commission fees for the VPP and battery cycling costs, are considered to estimate the net monthly cost saving that EV customers should realize.

This study applies a multi-period security constraint optimal power flow (MPSOPF) method, which is a stochastic form of power system optimization model that allows us to derive the optimal operational plan for the power system by reflecting stochastic inputs such as VRS. The stochastic forecast profiles of VRS are derived for each renewable site based on weather data using two-stage autoregressive moving average with exogenous variables (ARMAX) modeling and the Monte Carlo simulation method.

The remainder of this paper is structured follows. Section 2 describes the objective function and characteristics of the MPSOPF model, discusses the methodology of deriving VRS forecast profiles, and presents information regarding EV driving and charging patterns. Section 3 outlines the structure of the different DR programs and derives an optimal TOU rate and DR program. Section 4 analyzes the results of the study, and Section 5 discusses the conclusions and implications.

2. Methodology

2.1. The Power System Simulation Model

The MPSOPF model applied in this study is a type of security constraint optimal power flow model commonly used to simulate a power system. This model simulates a 24 h optimal dispatch plan that minimizes the operating costs of the power system from the perspective of day-ahead planning when security constraints are applied. The basic model structure seeks to derive a dispatch plan for each generator that minimizes energy and reserve costs under the various power system constraints regarding system security, network, contingency, and renewable energy variability as well as physical constraints, while meeting power demand requirements over a 24 h period.

There are two distinct characteristics by which the MPSOPF model used in this study differs from other common power flow models. First, this model can handle a stochastic form of input, so it can realistically analyze the impact of renewable energy generation on the power system by considering the forecasting error in the day-ahead scheme. Second, the amount of operating reserve required to ensure stability of the power system is derived from the model as internal solutions when uncertainties are imposed from various scenarios, such as uncertain renewable energy generation, demand, or contingency. These features enable the MPSOPF model to realistically reflect the variable and uncertain characteristics of renewable energy generation and analyze the costs of operating a power system with high levels of VRS.

Equation (1) shows the simplified objective function of the MPSOPF model. This objective function consists of four components: generation cost, contingency reserve cost, load-following reserve, and load-shedding costs. The MPSOPF model derives an optimal dispatch plan that minimizes these four cost components. [14,15] The detailed definition of variables is provided in the Table A1 in the Appendix A.

$$
\begin{aligned}
\min_{G_{itsk}, R_{itsk}, LNS_{jtsk}} \sum_{t\in T}\sum_{s\in S}\sum_{k\in K} \pi_{tsk}\{ \sum_{i\in I}[C_{G_i}(G_{itsk}) + Inc^{+}_{its}(G_{itsk} - G_{itx})^{+} \\
Dec^{-}_{its}(G_{itc} - G_{itsk})^{+}] \sum_{j\in J} VOLL_j LNS(G_{tsk}, R_{tsk})_{jtsk}\} \\
+ \sum_{t\in T}\rho_t \sum_{i\in I}[C^{+}_{R_{it}}\left(R^{+}_{it}\right) + C^{-}_{R_{it}}\left(R^{-}_{it}\right) + C^{+}_{L_{it}}\left(L^{+}_{it}\right) + C^{-}_{L_{it}}\left(L^{-}_{it}\right)] \\
\sum_{t\in T}\rho_t \sum_{s_2\in S^t}\sum_{s_1\in S^{t-1}}\sum_{i\in I^{ts_2 0}}\left[Rp^{+}_{it}(G_{its_2} - G_{its_1})^{+} + Rp^{-}_{it}\left(G_{its_2} - G_{its_1}\right)^{+} + f_s(p_{sc}, p_{sd})\right]
\end{aligned}
\qquad (1)
$$

The power system network in Jeju Island shown in Figure 1 is chosen for this study. Jeju Island has a population of 604,000, is popular with tourists from neighboring countries, and is renowned for its natural scenery and clean environment. To maintain a clean environment, the island's administration has implemented an aggressive agenda to replace fossil fuel power plants with renewable energy sources, specifically solar PV and wind, and displace conventional vehicles with EVs. Therefore, Jeju Island is a suitable case to analyze the impact of an EV DR program on a power system with high levels of renewable sources [1].

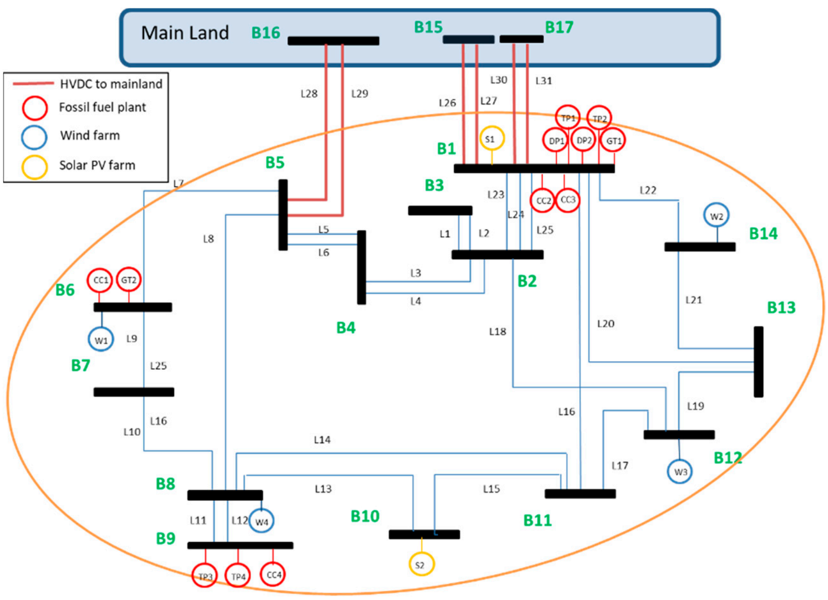

Figure 1. Power system network in Jeju Island (17-bus system).

The cost data is from the Korea Power Exchange (KPX) database of Electric Power Statistics Information System (EPSIS) [16] and reference costs used in this study are 40.5 USD/Gcal for natural gas and 53.9 USD/Gcal for oil. These unit heat costs for each fuel type are applied to cost functions of each generator to derive the generation cost of given power output. These costs are typically stable in Korea as they are in the long-term contract, so the cost data acquired from the Korea Power Exchange is used extensively. The original cost data is in KRW, and all cost results are converted to USD by apply 1200 KRW/USD ratio based on the official conversion ratio reported on 3 March 2020.

2.2. Model for Renewable Generation Forecasting

The wind and solar PV generation forecast profiles are estimated based on wind speed and solar radiation data from 2016 to 2018 from the Korea Meteorological Administration. Equations (2) and (3) below show the structure of the solar radiation and wind speed estimation models, respectively, based on the two-stage ARMAX model. The first stage uses deterministic information such as temperature and seasonal cycles to estimate the seasonal and temperature effect in wind speed and solar radiation, and the second stage takes the residual term of the first stage to estimate additional parameters through autoregressive moving average (ARMA) time series analysis [17,18]. This two-stage ARMAX model can be interpreted as capturing the variability of wind speed and solar radiation in the first stage and the uncertainty of the forecasting error in the second stage.

Stage 1: Deterministic part(Ordinary Least Square (OLS))

$$log(\text{Wind}_{t,i} + 1) = f_D\Big(\text{Deter mini stic Cycles}_{t,i},\ \text{Temperature}_{t,i}\Big) + \nu_{t,i} \tag{2}$$

where Deterministic $\text{Cycles}_{t,i}$ is a one-year, half-year, 24 h, and 12 h sine and cosine curve, and $\nu_{t,i}$ is the residual of the Stage 1 ordinary least squares estimation function.

Stage 2: ARMA part

$$(1 - \sum_{i=1}^{p} \alpha_i L^i)v_t = (1 + \sum_{j=1}^{q} \theta_j L^j)\varepsilon_t \tag{3}$$

where ε_t is the white noise residual of the Stage 2 ARMA estimation function.

Table 1 show the two-stage ARMAX estimation results of Wind Site 1, respectively. Pseudo R2, which indicates the explanatory power of the model that includes both Stage 1 and Stage 2, is 0.734 for the Wind Site 1 model.

Once the wind speed and solar radiation models are estimated for each wind and solar farm, the Monte Carlo simulation method is applied to create 1000 forecast profiles. Based on the covariance matrix of white noise residuals in Stage 2 of each econometric model, the simulation produces a random white noise residual assuming a normal distribution with variances along the covariance matrix, which results in 1000 wind speed and solar radiation forecast profiles. These generated forecast profiles are based on a variance-covariance matrix at each point, and therefore reflect spatial correlation for the six sites.

The set of 1000 wind speed and solar radiation forecast profiles is converted to wind power and solar power profiles using conversion formulae. Based on the 1000 solar and wind generation forecast profiles, five representative profiles are selected to simplify the profile information and reduce the computational burden for the MPSOPF model. Of the five profiles, the middle profile is the median, the second and fourth profiles indicate the +1 and −1 standard deviations from the median, and the top and bottom profiles are the +2 and −2 standard deviations from the median. These five chosen profiles cover 95% variability of total VRS profiles as shown in Figure 2.

Table 1. Two-stage ARMAX (autoregressive moving average with exogenous variables) estimation results for Wind1 (Hanlim).

Stage 1: OLS Model			Stage 2: ARMA Model		
Variable	**Coefficient**	***t*-Value**	**Variable**	**Coefficient**	***t*-Value**
Intercept	1.22258	208.66	constant	-4.1×10^{-5}	0
Cosine_year	0.14264	17.41	MA1	0.27082	38.02
Sine_year	0.02394	4.49	MA2	0.04158	6.1
Cosine_half year	−0.03084	−7.01	MA3	0.01328	1.97
Sine_half year	0.00414	0.87	MA4	0.008712	1.3
Cosine_day	−0.12054	−29.11	MA5	0.004728	0.71
Sine_day	−0.08894	−21.45	AR1	0.93123	261.22
Cosine_half day	0.00564	1.42	AR24	0.03472	5.6
Sine_half day	0.06246	15.67			
CDD [1]	0.03825	16.66			
HDD [2]	0.01441	13.06			
R2: 0.151			Pseudo R2: 0.734		

[1] CDD (cooling degree day) = max (temperature –24 °C, 0), [2] HDD (heating degree day) = max (18 °C temperature, 0).

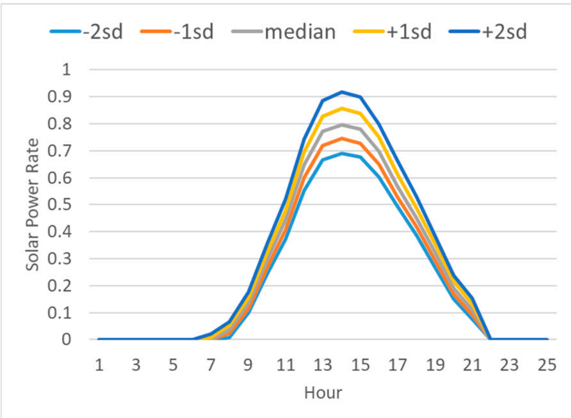

(**a**)

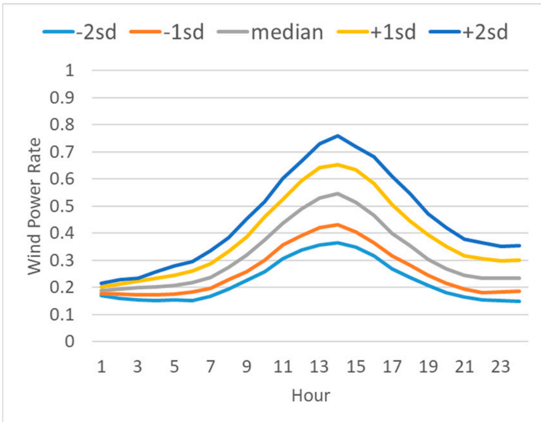

(**b**)

Figure 2. The five representative forecast profiles for sites Solar1 and Wind1: (**a**) Solar1 (Jeju City); (**b**) Wind1 (Hanlim).

Based on the estimated forecast profiles, we estimated the net load patterns for Jeju Island for 2019 and 2030. As shown in Figure 3, the net load in 2019 shows insignificant variability and uncertainty, although some duck curve characteristics can be observed. However, the net load in 2030 shows a severe duck curve, which causes a negative net load for the median profile. This could lead to a situation in which excess renewable energy must be returned to the mainland.

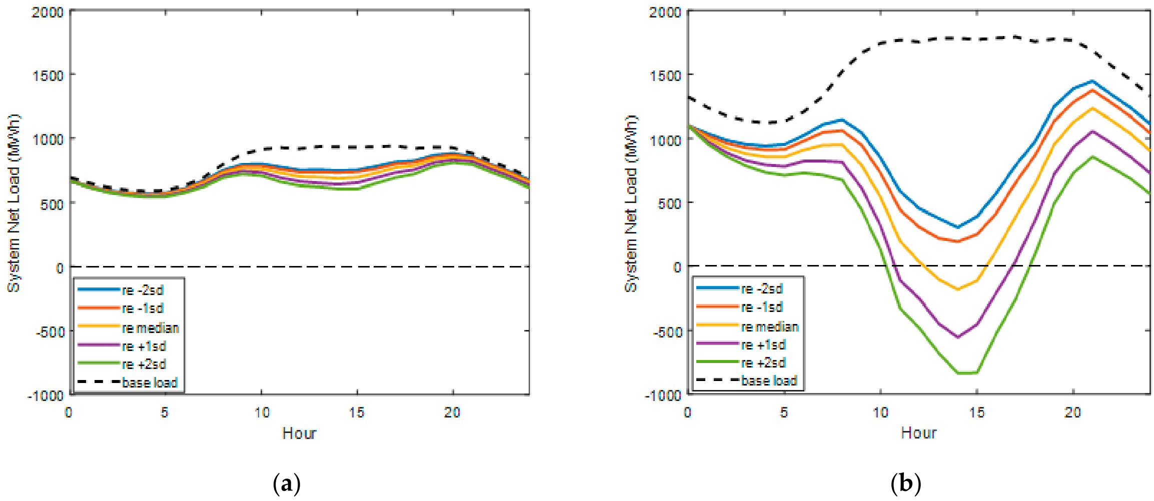

Figure 3. Forecasted net load for peak days in Jeju Island in 2019 and 2030: (**a**) 2019; (**b**) 2030.

2.3. Assumptions for Electric Vehicle (EV) Driving and Charging Patterns

To estimate the potential economic value of an EV DR program, it is important to impose realistic constraints for charging and driving patterns of EVs in the simulation. Figure 4a shows a profile of the average charging ratios among all EVs in Jeju Island. This profile is a weighted average of fast- and slow-charging profiles, with ratios of 9% to 91%, and an average charging duration time of 6.2 h for slow charging and 0.5 h for fast charging [19,20]. The aggregated charging ratio profile increases during the night from 7 pm to 5 am, when customers can take advantage of low electricity rates, and increases moderately from 11 am to 3 pm, when demand is generally highest. Figure 4b illustrates the hourly profile of the percentage of the total number of cars on the road in Jeju Island. The profile spikes during commuting hours from 7 am to 10 am and 6 pm to 9 pm and shows a moderately high percentage during the day.

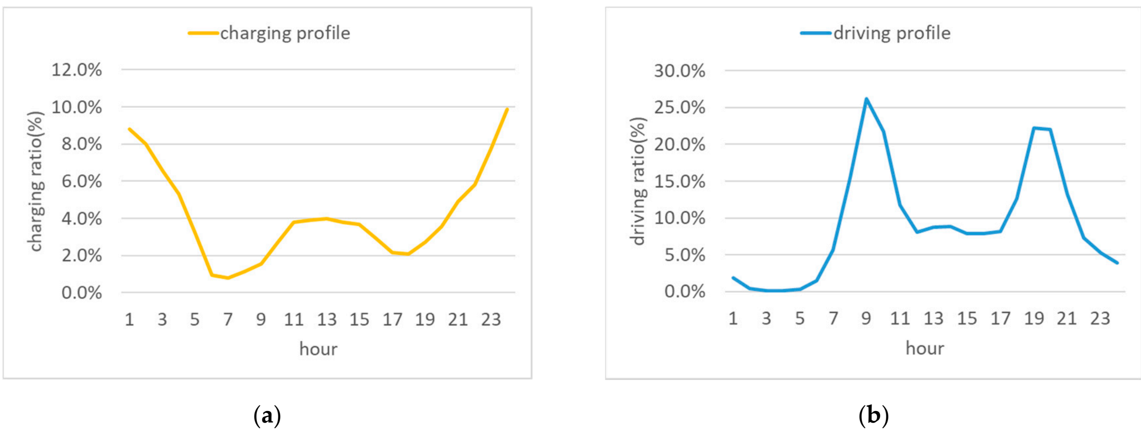

Figure 4. Charging ratio profile and driving profile of EVs for Jeju Island: (**a**) charging ratio profile; (**b**) driving profile.

3. Scenario Setup

3.1. Construction of Scenarios

Table 2 summarizes the structure of the four scenarios used in this study to estimate the potential value of an EV DR program. The first scenario (Case 1) is an estimate of the operating cost of the power system when the current EV demand pattern is maintained. The second scenario (Case 2) measures the impact of the EV DR program under a TOU tariff. The third scenario (Case 3) estimates the impact of EV demand when it is directly controlled by an aggregator using VPP technology; in this case, an aggregator uses a cyber-physical network to manage the aggregated EV DR resources as a virtual power plant under a direction from a system operator. Case 3 allows only the purchase of energy from the grid (grid-to-vehicle, G2V) and is referred to as VPP1. The fourth scenario (Case 4) assumes a smart control like VPP1 but allows both the G2V and vehicle-to-grid (V2G) and is referred to as VPP2. All four cases are analyzed in 2019, under moderate VRS levels, and in 2030, under high VRS levels.

Table 2. Structure of the scenarios.

Case Name	Description		Level of Demand Control	DR Participation Rate of EV
	Jeju Island in 2019 (Low VRS and EV)	Jeju Island in 2030 (High VRS and EV)		
Case 1: No Control	Current EV electricity consumption pattern		No control	10% 25% 50% 75% 100%
Case 2: TOU	EV charging pattern under TOU tariff		Passive control	
Case 3: VPP1 (G2V only)	Smart EV charging control by VPP		Active control	
Case 4: VPP2 (G2V + V2G)	Smart charging and discharging control by VPP		Highly active control	

This analysis has three key objectives. The first objective is to analyze how the value of the DR program differs with varying levels of control over EV demand. The level of control for EV demand increases with each case, ranging from no control in Case 1 to highly active control in Case 4. The second objective is to determine how the value of the EV DR program changes with varying levels of renewable energy. To analyze this, the impact of EV demand is estimated for 2019 and 2030, with ratios of renewable energy capacity to peak demand of 46% and 210%, respectively. The third objective is to estimate the impact of different EV participation rates on the cost of supplying electricity and to see the actual compensation and cost that can be incurred to each EV customer by providing a DR service to the grid.

A key characteristic of Case 1 is that the current EV charging pattern will be maintained until 2030, while in Case 2, the price elasticity of EV demand will be applied when determining the daily demand pattern under a TOU tariff. Case 3 assumes that EVs are connected to the grid at all times when they are not operating, and the aggregated charging power rate is determined based on the composition ratio of 7:2:1 for portable, slow, and fast chargers, respectively. A high portable charger rate strengthens the assumption that customers have high accessibility to the grid. In addition, it is assumed that VPP scenarios can provide not only energy but also ancillary services to the grid as they are optimally controlled based on the direction of a system operator. In Case 4, the available capacity of EV batteries for V2G capability is set at 70% to maintain performance and optimize battery life.

Table 3 summarizes the conditions and assumptions related to the technical characteristics of EVs separately in 2019 and 2030. The daily average driving distance and the average fuel efficiency are 52 km/day and 5.43 km/kWh, respectively, and by combining the two values, the daily average EV energy usage is computed as 9.39 kWh. The average EV battery capacity is set at 45.2 kWh for 2019 and 69.3 kWh for 2030 by assuming an average annual capacity increase of 4% due to advances in technology. If the current EV deployment plan for Jeju Island is achieved, the aggregated battery capacity will be approximately 1065 MWh in 2019 and 26,132 MWh in 2030, and the total daily electricity consumption by EVs will be approximately 247 MWh in 2019 and 5935 MWh in 2030. Projected figures in 2030 of Table 3 are mainly based on [1,2,5,20–23].

Table 3. EV characteristics in 2019 and 2030.

Variables	2019	2030	Unit
Average daily driving distance	52	Same	km
Average fuel efficiency	5.43	Same	km/kWh
Average daily electricity consumption	9.39	Same	kWh
Average battery capacity	45.2	69.3	kWh
Average daily driving hours	2.19	Same	hour
Composition of chargers by charging speed (portable:slow:fast)	7:2:1	Same	–
Total number of EVs	23,667	377,217	–
Aggregated EV battery capacity	1065	26,132	MWh
Total daily electricity consumption by EVs	247	5935	MWh
Depth of discharge of battery	70%	Same	–
Roundtrip battery efficiency	90%	Same	–

3.2. Estimation of EV Electricity Demand under a Time-of-Use (TOU) Program

Figure 5 illustrates the three-level design of the TOU program used in this study based on the net load in 2019 and 2030. Currently, TOU programs in Korea have three-level structures with different schemes to meet the load pattern of each season. They are commonly built with 10 h of low-rate supply, 8 h of mid-rate supply, and 6 h of high-rate supply. The proposed TOU structures in 2019 and 2030 are designed based on these current conditions.

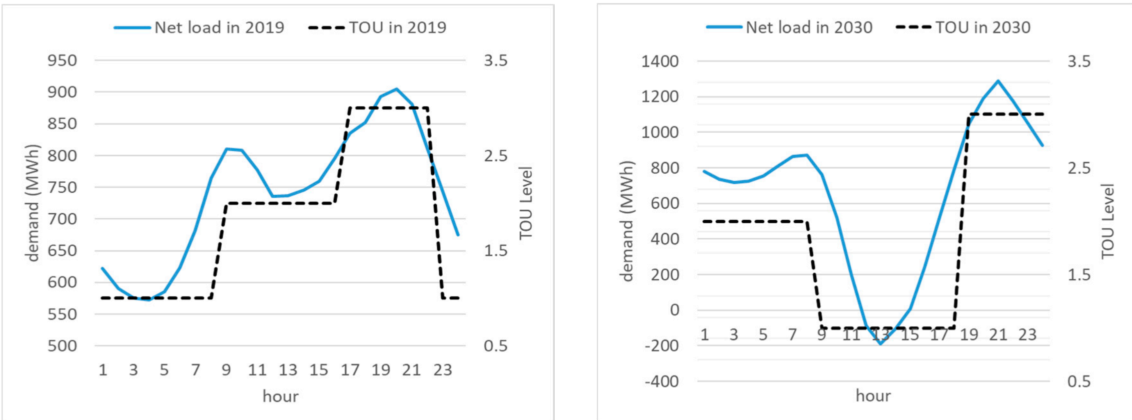

(**a**) (**b**)

Figure 5. Time-of-use (TOU) structures based on the net load in 2019 and 2030: (**a**) 2019; (**b**) 2030.

Figure 6a,b illustrate the estimated demand pattern of the EV DR under the TOU programs presented above. Research on how electricity demand responds to a TOU tariff is limited, and it is difficult to predict this response due to the lack of data and uncertainty in customers' behaviors. Therefore, based on Reference [24], it is assumed that the DR demand pattern under TOU is the aggregation of three separate demand profiles incurred by three rate segments, which follows a truncated normal distribution with different peak levels.

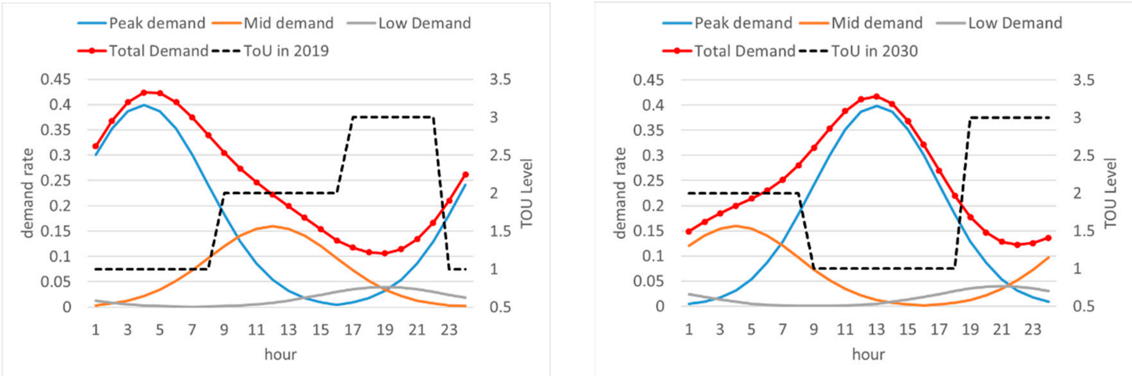

(**a**) (**b**)

Figure 6. Electricity demand profiles responding to a TOU program in 2019 and 2030: (**a**) 2019; (**b**) 2030.

The resulting demand pattern under the TOU program is derived by superimposing the demand profiles in the form of a standard normal distribution with three ratios adjusted for high-, mid-, and low-rate segments. The ratios for each segment are determined based on actual demand ratios in each segment for Jeju Island: 54% in the low-rate segment, 33% in the mid-rate segment, and 13% in the high-rate segment [19]. Therefore, by imposing these segment demand ratios, the actual price elasticity of demand for EVs is reflected in the TOU program demand pattern.

Figure 7 shows how the pattern of the net load will change if demand from the TOU program is introduced in 2019 and 2030. Although the 2019 results do not show a significant impact from the TOU program due to a lack of electricity demand from EVs, the 2030 results reduce the gap between the lowest and highest demand periods by actively raising demand during the duck curve hours. This shows that the TOU program helps to improve the efficiency of the power system by mitigating the severe duck curve problem.

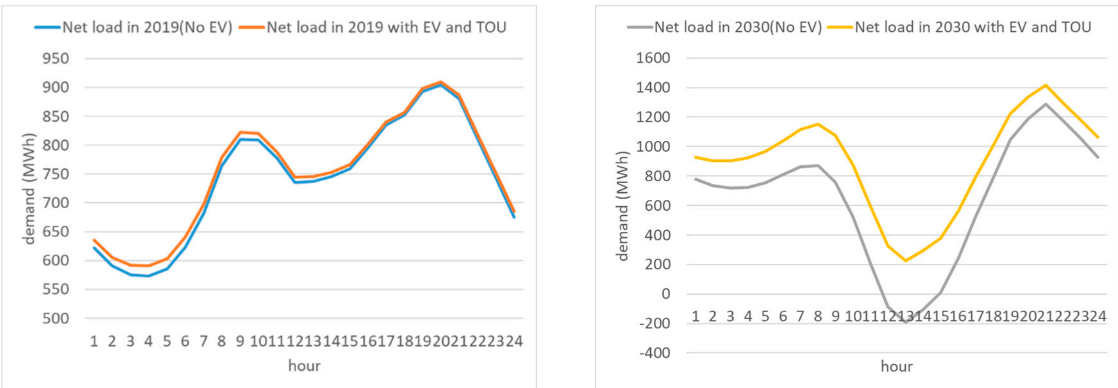

(**a**) (**b**)

Figure 7. Net load changes with EV demand affected by a TOU program in 2019 and 2030: (**a**) 2019; (**b**) 2030.

4. Results Analysis

4.1. The Impact of an EV Demand Response (DR) under Low Variable Renewable Sources (VRS) Level (2019)

Figure 8 shows the 24 h expected dispatch profiles by generation sources for peak day demand in 2019. It can be seen that energy inflow from the mainland through High Voltage Direct Current(HVDC) lines, diesel power, and thermal power provide electricity for base-load demand, and combined-cycle thermal power and gas turbine power are employed to meet peak demand in Jeju.

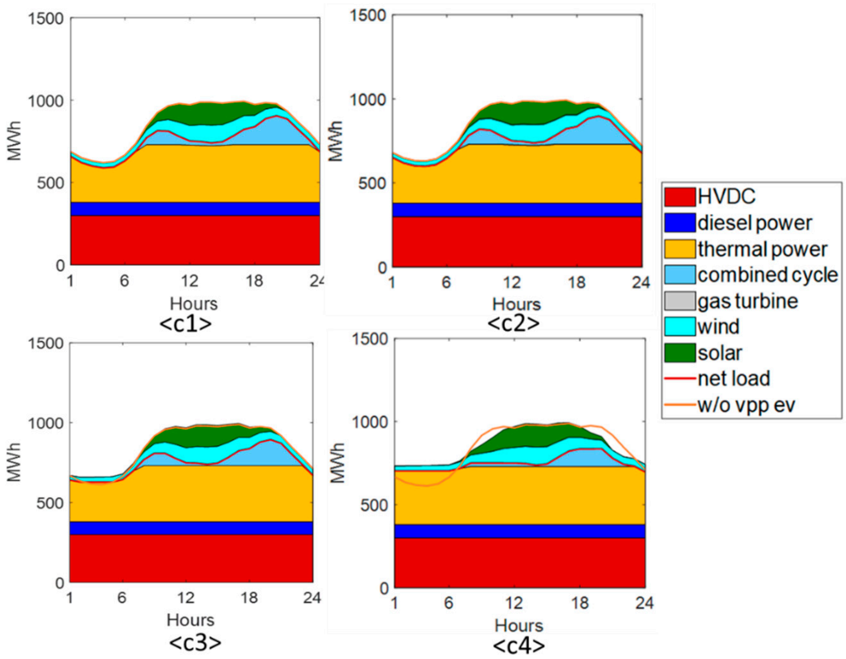

Figure 8. Expected dispatch profiles for summer peak day in 2019.

Case 1 shows that high renewable energy generation in Jeju Island is causing a moderate duck curve at peak hours. In Case 2, as the size of the EV demand resource is small, the effect of the TOU program is not apparent. If the program is smartly managed by a VPP, as in Case 3, EV demand increases in the early morning hours between 1 am and 4 am, utilizing inexpensive generation from TP. EV demand is marginal in Case 3 because the amount of energy consumed daily for each EV is not high in 2019.

In Case 4, the colored area above the base demand line (orange line) indicates that EVs are purchasing energy, and the area below the demand line means that EVs are injecting energy back into the grid. Case 4 shows more active charging during the early morning hours, when energy is inexpensive, and more active discharging during the peak hours between 11 am and 7 pm, when energy is expensive. The amount of load shifting is much larger than in Case 3 because EVs fully utilize their battery capacity to effectively shift load. As a result, the duck curve problem is largely mitigated.

Table 4 summarizes the daily power generation and reserve capacity required for the summer peak day in 2019. Renewable generation and conventional generation are noted as expected values because the amount of generation varies stochastically depending on renewable generation and contingency scenarios; meanwhile, the reserve amount is noted as an actual value as this is the reserve amount necessary to guard against all uncertain scenarios in the simulation.

Table 4. Daily generation and reserve for a summer peak day in 2019.

MWh/day	c1_2019	c2_2019	c3_2019	c4_2019
Wind generation	1451.6	1451.6	1464.8	1463.0
Solar PV generation	1130.1	1130.1	1130.6	1130.4
Conventional generation	17,923.2	17,920.2	17,908.7	17,982.2
Total reserve	4899.0	4887.2	3295.4	1172.9
Load-following reserve	2731.7	2719.9	1741.0	748.6
Contingency reserve	2167.2	2167.2	1554.4	424.3
Load shedding	0.1	0.1	0.1	0.0

The results for Case 2 are similar to those for Case 1. The total reserve requirement decreases slightly due to the TOU program's marginal contribution to the duck curve problem; however, the Case 3 scenario shows that the amount of conventional generation and reserve requirements are significantly reduced. The reduction in conventional generation is due to accommodating more renewable generation as EV electricity demand helps to mitigate variability from renewable sources; the reduction in the reserve requirement is due to the use of EV DR as ancillary service resources.

Case 4 shows a significant reduction in the amount of reserve required, but conventional energy generation increases. This shows that EV DR could be used more effectively for ancillary services in the presence of V2G technology; however, electricity demand increases due to the round trip inefficiency of EV batteries charging and discharging, which results in an increase in conventional generation.

Table 5 summarizes the daily operating costs including generation and reserve costs for peak day demand in 2019. Case 2 shows a marginal reduction in the generation cost compared to Case 1 and does not achieve a significant reduction in the reserve cost. Case 3 shows a meaningful reduction in both generation and reserve costs—approximately 6200 USD/day and 5500 USD/day, respectively. The proportion of the total daily reserve cost is less than 1% of the total operating cost, but the reserve cost reduction takes approximately 47% of the total operating cost reduction which is composed of a 39.5% reduction in reserve cost and a 0.3% reduction in generation cost.

Table 5. Daily operating costs of generation and reserve for a summer peak day in 2019.

1000 USD/day [1]	c1_2019	c2_2019	c3_2019	c4_2019
Generation cost	1794.2	1791.8	1788.0	1779.3
Total reserve cost	13.9	13.9	8.4	2.9
Load-following reserve cost	8.1	8.0	4.7	1.9
Contingency reserve cost	5.8	5.8	3.8	1.0
Load shedding * Value of lost load	0.7	0.7	0.7	0.1
Total operating cost	1808.8	1806.3	1797.1	1782.3
Generation cost reduction from c1	–	0.1%	0.3%	0.8%
Total reserve cost reduction from c1	–	0.0%	39.5%	79.0%
Total operating cost reduction from c1	–	0.1%	0.6%	1.5%

[1] A currency exchange rate of KRW 1200/USD is applied to all costs in this study.

Case 4 shows a 1.5% decrease in the total operating cost compared to Case 1, comprised in part of a 0.8% decrease in generation cost and a 79% decrease in reserve cost. The total operating cost reduction from the VPP2 program in Case 4 is almost three times higher than in Case 3. This is achieved by significant reductions in both generation and reserve costs. The reserve cost is reduced by approximately 79% compared to Case 1, which shows that EV demand controlled by the VPP2 program can provide effective ancillary service capacity for renewable sources.

4.2. The Impact of an EV DR Program under High VRS Level (2030)

Figure 9 shows the expected 24 h dispatch profiles for the summer peak day peak day in 2030. Case 1 shows that the Jeju Island power system has the problem of negative net load from 12 pm to 4 pm due to concentrated generation from renewable sources, particularly solar PV. In Case 2, EV DR under the proposed TOU program resolves the negative net load problem by increasing demand during duck curve hours. In Case 3, the demand control under the VPP1 program effectively resolves the duck curve by increasing EV demand during peak hours and reducing it during off-peak hours, providing a reliable and cost-effective power supply. Case 4 further shifts the net load supplied by expensive combined-cycle units to more cost-effective thermal power units.

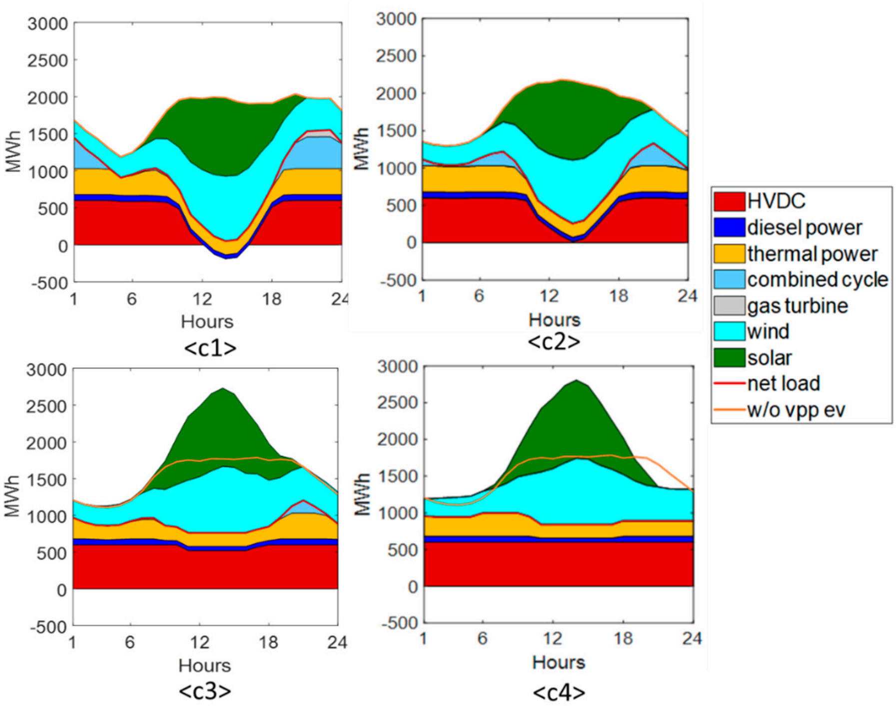

Figure 9. Expected dispatch profiles for a summer peak day in 2030.

Cases 3 and 4 do not display significantly different results. This is because this analysis assumes 100% EV demand participation. The planned number of EVs by 2030 is significant compared to the planned power system capacity; therefore, most power supply issues would be resolved if all EV customers were to participate in the VPP1 program, even with very high VRSs. Hence, the VPP2 program does not greatly contribute additional benefits. To analyze the impact of the VPP2 program, the effect of various EV participation rates are assessed in Section 4.4.

Table 6 summarizes the daily amount of generation and reserve needed in the peak summer day in 2030, characterized by a high renewable capacity situation. In Case 1, significant load shedding occurs with severe negative net loads. To achieve a feasible optimal solution, the MPSOPF assigns 10,000 USD/MWh, or 100 times the normal peak SMP, as the value of lost load, and allows load shedding if it is economically feasible even with high costs.

Table 6. Daily generation and reserve for a summer peak day in 2030.

MWh/day	c1_2030	c2_2030	c3_2030	c4_2030
Wind generation	12,159.3	12,233.8	12,522.9	12,522.9
Solar PV generation	8654.3	8655.1	8679.5	8679.5
Conventional generation	21,683.7	21,666.2	21,355.8	21,803.1
Total reserve	25,907.9	28,881.8	8721.1	487.4
Load-following reserve	17,136.3	19,101.1	5786.2	415.2
Contingency reserve	8771.6	9780.7	2935.0	72.3
Load shedding	59.8	0.1	0.0	0.0

In Case 2, most of the load shedding problem is resolved as demand control under the TOU program effectively increases charging consumption during the hours that the power system suffers from a negative net load. Case 3, with very high EV demand capacity under the VPP1 program, accommodates substantially more wind energy compared to Case 1 by effectively mitigating wind variability; as a result, the amount of reserve needed is reduced to almost one-third of that in Case 1, and the amount of conventional generation is also reduced.

Case 4 is similar to Case 3 due to the high level of EV participation in the demand program. However, Case 4 further reduces 95% of reserve required in Case 3. This means that a VPP2 program with V2G capability replaces reserve capacities effectively by actively reducing the variability of renewable energy sources.

Table 7 summarizes the daily operating costs of generation and reserve in 2030. Case 2 reduces the total operating cost by 23.9%, mainly due to a reduction in generation cost and the cost related to load shedding caused by the serious duck curve. In Case 3, both generation and reserve costs are considerably reduced, which leads to a total operating cost reduction of 31.9% compared to Case 1. In Case 4, generation cost is slightly increased but reserve cost is significantly decreased compared to Case 3, which shows that the optimal use of EV demand under a VPP2 program focus more on mitigating the variability of renewable energy sources and less on load shifting.

Table 7. Daily operating costs of generation and reserve for a summer peak day in 2030.

1000 USD/day	c1_2030	c2_2030	c3_2030	c4_2030
Generation cost	2785.9	2545.7	2329.2	2339.2
Total reserve cost	82.3	91.4	30.5	2.3
Load-following reserve cost	54.3	60.2	20.2	2.1
Contingency reserve cost	28.0	31.2	10.3	0.2
Load shedding * Value of lost load	597.8	0.9	0.4	0.0
Total operating cost	3466.0	2638.0	2360.1	2341.5
Generation cost reduction from c1	–	8.6%	16.4%	16.0%
Total reserve cost reduction from c1	–	−11.1%	62.9%	97.2%
Total operating cost reduction from c1	–	23.9%	31.9%	32.4%
Total operating cost reduction without load shedding from c1	–	8.1%	17.7%	18.4%

Figure 10 illustrates the monthly cost reduction per EV by the different DR programs in 2019 and 2030. In 2019, the cost reduction by the TOU program is limited, while the benefits from the VPP2 program are almost double that of the VPP1 program. The reserve cost saving is almost as large as generation cost saving in both VPP1 and VPP2 programs, which shows that it is an important contribution that EV DR can provide.

In 2030, the cost savings per EV in Case 2 and Case 3 are increased as EV DR can effectively contribute to solve the problem caused by high VRS sources. However, the cost saving per EV in Case 4 is not very different to the cost saving of Case 3 and it is actually reduced compared to that in 2019. This is because the number of EV in 2030 is too large to the size of the system, so most problems are solved by VPP1 and only little additional cost reduction is achieved by V2G.

In order to estimate the true contribution that each EV DR resource can provide to the system with varying VRS penetration, we analyzed the cost saving with the same number of EVs in 2019 and 2030. To equalize the number of EVs in 2019 and 2030, we assumed 6.2% of total EVs participate in the DR program in 2030. As shown in Figure 11, monthly cost saving in 2019 are 2.9 USD/month, 13.8 USD/month, and 31.5 USD/month for Case 2, Case 3, and Case 4, respectively, whereas those in 2030 are 28.5 USD/month, 65.8 USD/month, and 202.1 USD/month, respectively. This shows that the value of the EV DR is much higher in a power system with a high penetration of VRS sources because the EV DR can effectively reduce the high operating costs caused by the variability and uncertainty of VRS.

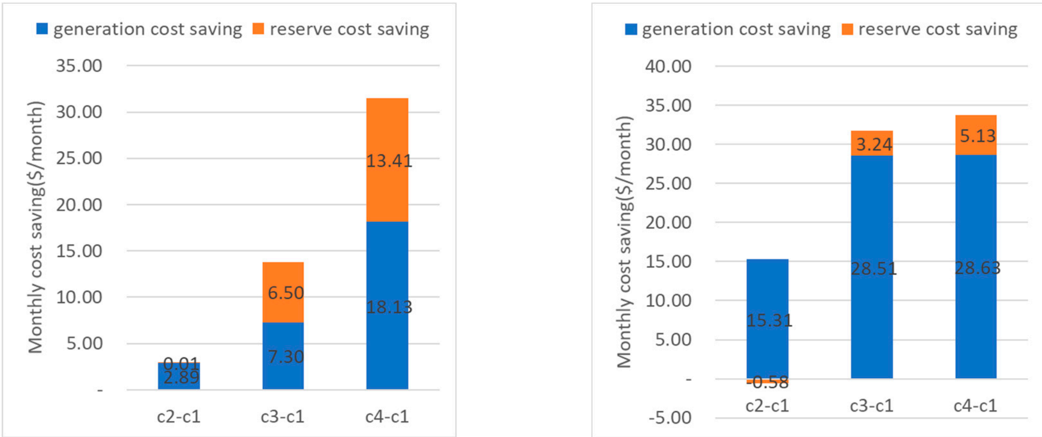

(**a**) (**b**)

Figure 10. Monthly cost saving per EV under varying DR programs in 2019 and 2030: (**a**) 2019; (**b**) 2030.

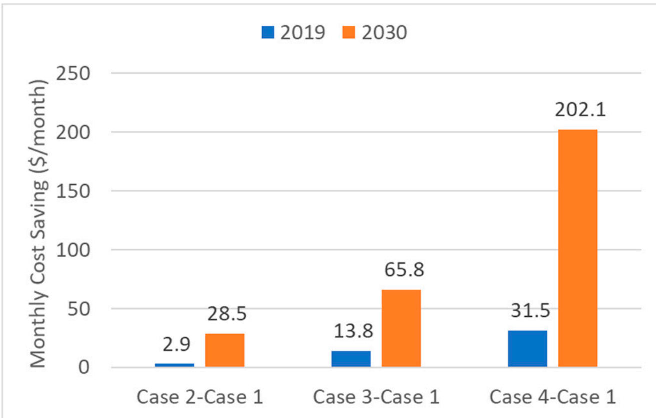

Figure 11. Adjusted monthly cost saving per EV customer in 2019 and 2030.

The implications of the scenario analyses in 2019 and 2030 can be summarized in two main points. First, EV demand is an effective resource to enhance the reliability of a power system that is undermined by a high penetration of renewable energy sources. In 2030, when the capacity of VRS increases to 210% of the peak demand, EV DR reduces the operating cost significantly by effectively mitigating a severe duck curve problem. Second, DR under a VPP program significantly outperforms a TOU program; however, the additional benefit from V2G technology in the VPP2 program is not significant when the size of the EV demand resource is large relative to the size of the power system, because most existing issues are resolved by the VPP1.

4.3. Optimal Charging and Discharging Profiles of EVs by Different Control Structures

Figure 12 illustrates the optimal charging and discharging profiles of EVs by the four different demand control programs in 2019 and 2030. In 2019, the low net load hours are from 1 am to 6 am, therefore all DR programs attempt to shift load to these hours, but the magnitude differs. Both the TOU and VPP1 programs slightly increase EV demand during the low net load hours, while the VPP2 program, which fully utilizes the EV battery, shows a significant demand increase in the early morning and substantial V2G discharging in the hours when expensive combined-cycle plants are heavily used. The different charging profiles between the VPP1 and VPP2 programs show that V2G capability can more actively contribute to enhance the efficiency of power system operation.

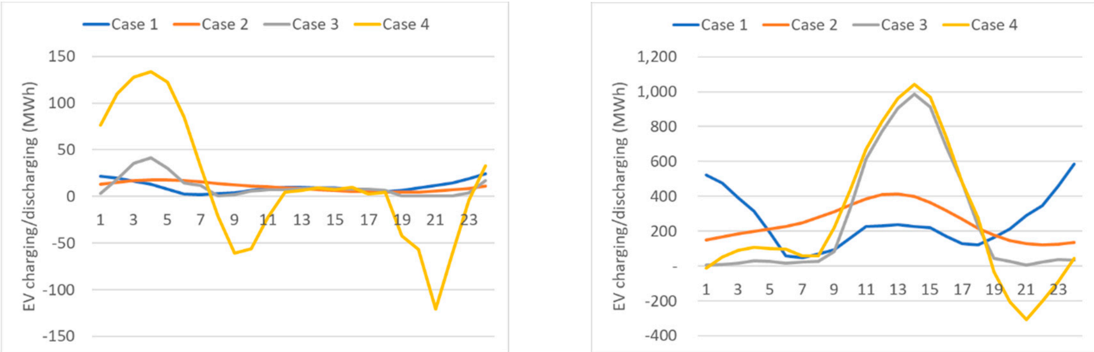

(**a**) (**b**)

Figure 12. Optimal charging/discharging profiles of DR programs in 2019 and 2030: (**a**) 2019; (**b**) 2030.

However, in 2030, demand increases for all four programs during duck curve hours, when generation from renewable sources is concentrated. DR under the TOU program slightly increases during the duck curve hours, but unlike the 2019 scenario, the charging profiles for the VPP1 and VPP2 programs are similar to each other. As discussed earlier, this is due to the large size of the EV resource in 2030: under a full participation scenario, V2G technology does not add additional value to improve the efficiency of the power system.

4.4. Net Cost Saving from the EV DR Programs by Varying the Participation Rate

As presented in Table 8, the ratio of EV hourly charging power capacity to peak demand is 1.58 under a 100% participation scenario in 2030. This means the possible amount of energy that an EV can charge in an hour is 1.58 times the peak demand of the system, which is very high and does not provide the analysis for a more realistic situation. Hence, we conducted an analysis with varying participation rates of 10%, 25%, 50%, and 75%. As seen in Table 8, the charging power capacity to peak demand ratio is 0.16 at 10% participation, which is a realistic level that can be achieved in the near future.

Table 8. Charging power capacity to peak demand ratio by various EV participation rates in 2030.

Participation Rate of EV Demand	10%	25%	50%	75%	100%
Charging Power Capacity to Peak Demand Ratio	0.16	0.30	0.79	1.18	1.58

Figure 13 shows the expected 24 h dispatch profiles for varying EV participation rates in 2030. Case 2 shows marginal changes with different participation rates, and as EV demand increases, the low net load slowly increases in duck curve hours. Case 3 shows significant improvement in the net load in duck curve hours as the participation rate increases. In Case 4, when the participation rate is at 25%, the net load profile differs significantly from that of Case 3, which shows the beneficial impact of V2G technology. However, the difference between Case 3 and Case 4 reduces as the participation rate rises.

Table 9 summarizes the monthly gross cost saving, induced cost, and net cost saving per EV for the TOU, VPP1, and VPP2 programs compared to Case 1 by varying participation rate in 2030. Four seasonal representative days are selected to derive the annualized cost saving based on an interpolation method. The results show that the lower the participation rate, the higher the per-EV benefit, because EV demand reduces the most expensive cost factors first if it is optimally used in the grid. Under a realistic 10% participation rate scenario, the cost saving from the TOU, VPP1, and VPP2 programs is 23.3 USD/month, 59.4 USD/month, and 185.3 USD/month, respectively.

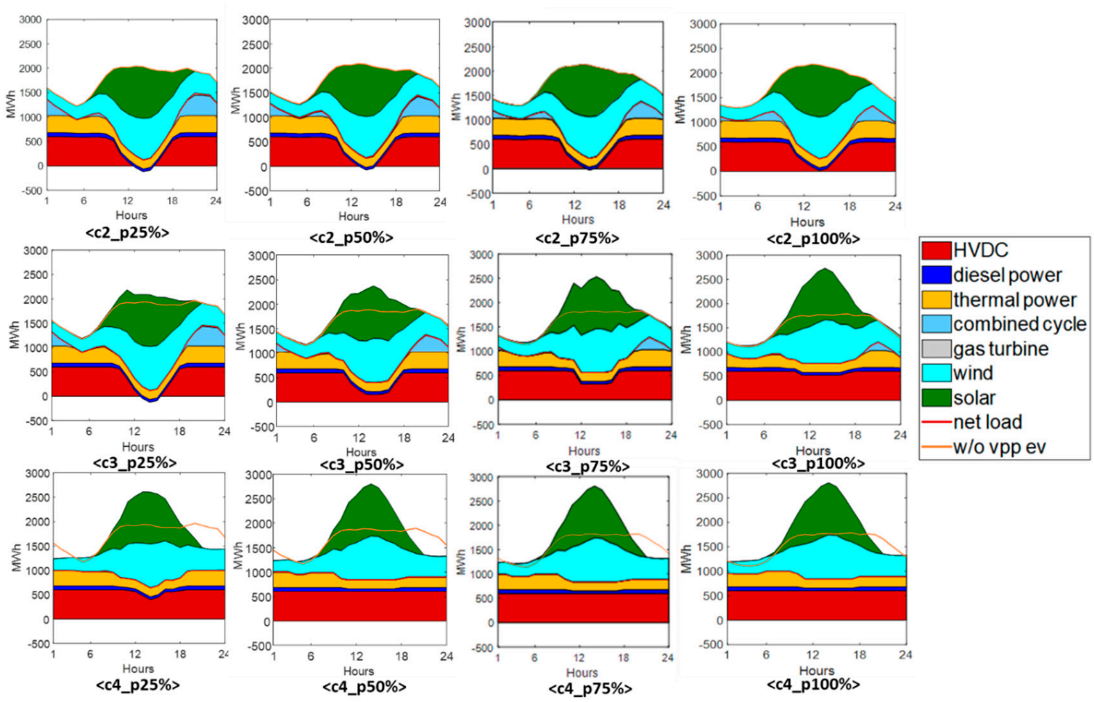

Figure 13. Expected 24-h dispatch profiles for varying EV participation rates in 2030.

Table 9. Monthly net cost saving per EV by varying participation rates (USD/month).

Participation Rate	Gross Cost Saving			Induced Cost			Net Cost Saving		
	TOU	VPP1	VPP2	TOU	VPP1	VPP2	TOU	VPP1	VPP2
10%	23.3	59.4	185.3	–	8.87	112.64	23.34	50.51	72.69
25%	18.3	47.7	131.9	–	8.87	92.31	18.27	38.79	39.63
50%	16.9	45.6	76.4	–	8.87	50.68	16.90	36.77	25.71
75%	15.6	37.4	51.2	–	8.87	31.32	15.64	28.53	19.90
100%	14.7	31.7	33.8	–	8.87	22.91	14.73	22.88	10.84

It should be noted that this monthly saving is not entirely realized by the consumer; additional costs related to providing the EV DR should be considered. There are three categories of additional costs.

First, a commission must be paid to the aggregator for operating my EV DR optimally through the VPP. Based on the current DR program in Korea, the average commission for EV demand is estimated at 8.87 USD/month (computed based on a capacity payment of 35.8 USD/kW, an energy payment of 7.1 cents/kWh, and a commission rate to total compensation of 30%) [25]. This amount is applied to the VPP1 program, which manages G2V only. It is assumed that the VPP2 program requires more sophisticated and active demand control, and thus, we double the commission. The commission cost is not relevant to the TOU program as the TOU does not require an aggregator.

Second, if EV batteries are actively utilized as DR resources, the wear-and-tear cost caused by frequent battery cycling should be considered. The battery cycling cost is estimated to be 118.3 USD/month at the 10% participation rate and 28.5 USD/month (computed based on an EV battery package cost of 300 USD/kWh, a battery life span of 10 years, a battery cycle life of 3000 cycles, and a 70% depth of discharge) at the 100% participation rate [26]. Figure 14 demonstrates the reason for varying battery cycling costs for different the participation rate scenarios. The black solid line shows the expected energy level in the battery and the red dashed line shows the maximum usable capacity, which is 48.5 kWh/vehicle after applying a 70% depth of discharge rate. The green and blue dashed lines show the possible boundary of battery energy levels caused by the uncertainty of renewable sources, reflecting that the battery actively charges or discharges to provide reserve capacity for renewable energy sources. It is estimated that a 10% participation case has a cycle of 0.93/day and a 100% participation case has a cycle of 0.22/day. In order to estimate purely additional battery cycling cost for providing DR service, battery cycling routinely occurring due to commuting is subtracted.

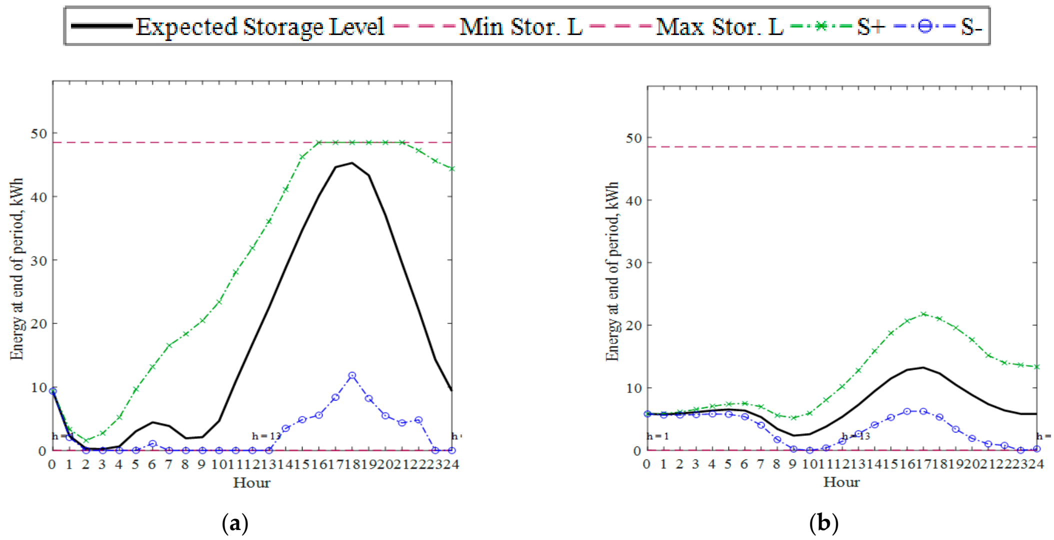

Figure 14. Average cycling pattern of an EV battery for 10% and 100% participation rates in 2030: (**a**) 10% participation; (**b**) 100% participation.

Third, the cost of inconvenience for customers in providing the DR service must be considered. Customers under a TOU program must voluntarily shift demand from time to time, and customers under the VPP1 and VPP2 programs are required to constantly connect their vehicles to the grid using portable chargers when not in operation. However, as this cost is subjective and difficult to quantify, we calculate the net cost saving for customers and discuss whether it is enough to offset the inconvenience of providing the DR service in the discussion.

Figure 15 highlights the gross cost saving and net cost saving in the four EV DR programs after considering the induced costs presented in Table 9. At a 10% participation rate, the VPP2 program has a substantial gross cost saving of 185.3 USD/month; however, with high battery cycling costs and a commission for an aggregator, the net cost saving is approximately 72.69 USD/month. The VPP1 program has a lower gross cost saving of 59.4 USD/month, but the aggregator commission is lower and there is no additional battery cycling cost incurred; thus, the net cost saving is 50.51 USD/month. The gross cost saving for the TOU program is much lower at 23.3 USD/month, but there is no additional cost; thus, the net cost saving remains at 23.3 USD/month.

While the analysis shows that the VPP2 program provides a significantly larger gross cost saving than the VPP1 program, the net cost saving reveals different results. As the EV participation rate increases, the net cost saving realized in the VPP2 program rapidly decreases due to decreased per-EV cost saving and high battery cycling costs. As a result, the net cost saving in the VPP2 program falls below that of the VPP1 program after the 25% participation rate is reached, and falls below the TOU program at the 100% participation rate.

The benefits to customers at the 10% participation rate in the VPP2 and VPP1 programs are much higher than those in the TOU program, and considering the monthly average EV energy cost of 29.1 USD/month (estimated based on an average EV energy consumption of 9.39 kWh/day, an average electricity rate of 0.096 USD/kWh, and a monthly fixed rate of 1.99 USD/month), the VPP2 and VPP1 programs allow customers to run EVs for a negative net payment; in other words, customers get paid to run EVs by participating in the program. This shows that even when considering the inconvenience costs of providing DR services, the incentives to participate can be sufficient if the cost saving that EV DR customers provide is correctly transferred to the service providers. The net benefit from the TOU program is not as large as those of the other programs, but customers can still reduce approximately 80% of their EV energy cost. In addition, considering that the TOU program is very easy to implement administratively and technically, this is also an effective alternative to incentivize EV DR to participate.

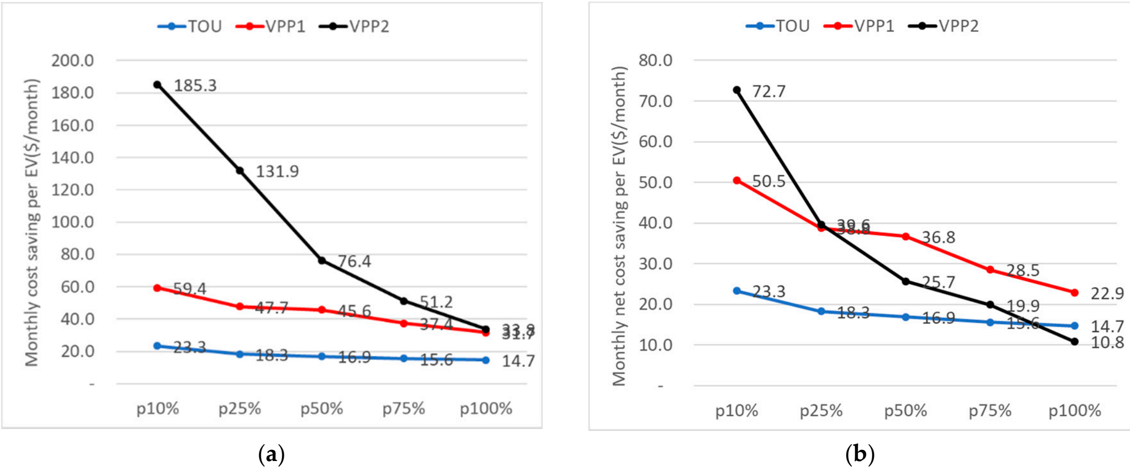

Figure 15. Monthly gross cost saving and net cost saving per EV by varying participation rates (USD/month): (**a**) gross cost saving; (**b**) net cost saving.

5. Conclusions

In this study, the economic values of various EV DR programs are assessed in a power system with different levels of VRS for Jeju Island, Korea. The main results that this study found can be summarized below.

First, the cost saving of an EV DR program is highly dependent on the level of VRS in the power system. In 2019, the cost savings that can be achieved by an EV customer for the TOU, VPP1, and VPP2 programs are 2.9 USD/month, 13.8 USD/month, and 31.5 USD/month, respectively; in 2030 with the same EV DR capacity, the cost saving is 28.5 USD/month, 65.8 USD/month, and 202.1 USD/month, respectively. The higher benefits in 2030, when the VRS capacity is higher shows that EV DR is more valuable as it effectively reduce the high operating cost caused by the high variability and uncertainty of VRS sources.

Second, at a reasonable 10% EV participation rate, the gross cost saving per EV customer is 23.3 USD/month, 59.4 USD/month, and 185.3 USD/month for the TOU, VPP1, and VPP2 programs in 2030, respectively. When the costs required to implement the programs are considered, such as aggregator commission and battery cycling costs, the net cost saving is reduced to 23.2 USD/month, 50.5 USD/month, and 72.7 USD/month, respectively. However, these net monthly cost savings are still higher than the average EV fuel cost of 29.1 USD/month, and the benefits from both the VPP1 and VPP2 programs are high enough to incentivize customers to join the DR program despite the inconveniences. The estimated benefit from the TOU program is marginally lower than the monthly fuel cost; however, it is the most easily implementable DR program and can potentially improve the efficiency of the power system, especially when coupled with critical peak pricing, to make EV demand more responsive to price.

Third, when the EV participation rate increases, the monthly cost saving per customer in the VPP2 program rapidly decreases and eventually becomes lower than that in the TOU program. This shows that the optimal DR program that can achieve maximum operating cost reduction will vary depending on the scale of EV demand.

An EV DR program can be an effective demand-side solution with high growth potential to mitigate the problems caused by high levels of VRS in the power system. Moreover, if the cost saving that EV DR can achieve in the system operation is effectively transferred to customers, EV owners will be sufficiently incentivized to participate in the DR program. This shows that implementing an appropriate DR program with an adequate compensation structure for customers will attract more DR customers to participate and this will help build a cost-efficient and reliable power system that can accommodate more green energy.

For future work, this study analyzed the value of EV demand resources in the Jeju grid which is approximately 1% of the national grid. To provide more valid evidence regarding the value of EV demand resources, this study must be extended to the national level by incorporating the national power grid and EV deployment plan.

Author Contributions: Conceptualization, W.J., S.C. and S.L.; methodology, W.J.; validation, W.J., S.C. and S.L.; formal analysis, W.J., S.L.; writing—original draft preparation, W.J.; writing—review and editing, S.C. and S.L. All authors have read and agreed to the published version of the manuscript.

Funding: This work was supported by the Ministry of Education of the Republic of Korea and the National Research Foundation of Korea (NRF-2018S1A5A8028620).

Acknowledgments: This research is partially based on the research report (19-25-03) from Korea Energy Economics Institute, but significantly improved and modified.

Conflicts of Interest: The authors declare no conflict of interest.

Appendix A

Table A1. Definition of variables in multi-period security constraint optimal power flow (MPSOPF).

Variables	Description
T	Set of time periods considered, n_t elements indexed by t
B	Set of buses in the system, n_b elements
S^t	Set of states in the system in period t, n_s elements indexed by s
K^{ts}	Set of contingencies in the system in period t and state s, n_c elements indexed by k
I^{tsk}	Set of generators in the system in period t, state s, and contingency k, n_g elements indexed by i
J^{tsk}	Set of loads in the system in period t, state s, and contingency k, n_l elements indexed by j
π_{tsk}	Probability of contingency k occurring, in state s, period t
ρ_t	Probability of reaching period t
G_{itsk}	Quantity of apparent power generated (MVA), active and reactive injections $(p_{i\,t\,sk} + \sqrt{-1}q_{i\,t\,sk})$
G_{itc}	Optimal contracted apparent power (MVA)
V^{tsk}	Set of voltages in period t, state s and contingency k, n_b elements for each bus in the system
θ^{tsk}	Set of angles in period t, state s and contingency k, n_b elements
p_{itsk}	Active power generated (MW), 0 refers to base case(s), n_g elements
p^c_{it}	Optimal contracted active power (MW), n_g elements
p^+_{itsk}, p^-_{itsk}	Upward/downward deviation from active power contract quantity for unit i in post-contingency state k of state s at time t, n_g elements
$C_G(\cdot)$	Cost of generating $(\cdot)$ MVA of apparent power
$Inc^+_{its}(\cdot)^+$	Cost of increasing generation from contracted amount
$Dec^-_{its}(\cdot)^+$	Cost of decreasing generation from contracted amount
$VOLL_j$	Value of lost load, ($)
$LNS(\cdot)_{jtsk}$	Load not served (MWh)
$R^+_{it} < Ramp_i$	$(max(G_{i\,t\,sk}) - G_{i\,t\,c})^+$, up reserves quantity (MW) in period t
$C^+_R(\cdot)$	Cost of providing $(\cdot)$ MW of upward reserves
$R^-_{it} < Ramp_i$	$(G_{i\,t\,c} - min(G_{i\,t\,sk}))^+$, down reserves quantity (MW)
$C^-_R(\cdot)$	Cost of providing $(\cdot)$ MW of downward reserves
$L^+_{it} < Ramp_i$	$(max(G_{i,t+1,s}) - min(G_{i\,t\,s}))^+$, load follow up (MW) t to $t + 1$
$C^+_L(\cdot)$	Cost of providing $(\cdot)$ MW of load follow up
$L^-_{it} < Ramp_i$	$(max(G_{i\,t\,s}) - min(G_{i,t+1,s}))^+$, load follow down (MW)
$C^-_L(\cdot)$	Cost of providing $(\cdot)$ MW of load follow down
$Rp^+_{it}(\cdot)^+$	Cost of increasing generation from previous time period
$Rp^-_{it}(\cdot)^+$	Cost of decreasing generation from previous time period
$\delta^+_{it}, \delta^-_{it}$	Upward/downward load-following ramping reserves needed from unit i at time t for transition to time $t + 1$
$\delta^{max+}_{it}, \delta^{max-}_{it}$	Upward/downward load-following ramping reserve limits for unit i
$f_s(p_{sc}, p_{sd})$	Value of the leftover stored energy in terminal states

References

1. Ministry of Trade, Industry and Energy (MOTIE). *The 8th Basic Plan for Long-Term Electricity Supply and Demand (2017~2031)*; MOTIE: Sejong, Korea, 2017.
2. Ministry of Trade, Industry and Energy (MOTIE). *The 3rd Basic Plan for Long-Term Energy Supply and Demand (2020~2040)*; MOTIE: Sejong, Korea, 2019.
3. Ueckerdt, F.; Brecha, R.J.; Luderer, G. Analyzing major challenges of wind and solar variability in power systems. *Renew. Energy* **2015**, *81*, 1–10. [CrossRef]
4. Baharvandi, A.; Aghaei, J.; Niknam, T.; Shafie-Khah, M.; Godina, R.; Nojavan, S. Bundled Generation and Transmission Planning Under Demand and Wind Generation Uncertainty Based on a Combination of Robust and Stochastic Optimization. *IEEE Trans. Sustain. Energy* **2018**, *9*, 1477–1486. [CrossRef]
5. Korea Energy Economics Institute (KEEI). *Modified CFI 2030 Plan to Implement Energy Self-Reliance Island*; KEEI: Ulsan, Korea, 2019.
6. Jeon, W.; Lamadrid, A.J.; Mo, J.Y.; Mount, T.D. Using deferrable demand in a smart grid to reduce the cost of electricity for customers. *J. Regul. Econ.* **2015**, *47*, 239–272. [CrossRef]
7. White, C.D.; Zhang, K.M. Using vehicle-to-grid technology for frequency regulation and peak-load reduction. *J. Power Sources* **2011**, *196*, 3972–3980. [CrossRef]
8. Zhang, L.; Li, Y. Regime-switching based vehicle-to-building operation against electricity price spikes. *Energy Econ.* **2017**, *66*, 1–8. [CrossRef]
9. Lyon, T.P.; Michelin, M.; Jongejan, A.; Leahy, T. Is "smart charging" policy for electric vehicles worthwhile? *Energy Policy* **2012**, *41*, 259–268. [CrossRef]
10. Ensslen, A.; Ringler, P.; Dörr, L.; Jochem, P.; Zimmermann, F.; Fichtner, W. Incentivizing smart charging: Modeling charging tariffs for electric vehicles in German and French electricity markets. *Energy Res. Soc. Sci.* **2018**, *42*, 112–126. [CrossRef]
11. Clairand, J.-M.; Bel, C.A.; Garcia, J.R.; Escrivá-Escrivá, G. Impact of Electric Vehicle Charging Strategy on the Long-Term Planning of an Isolated Microgrid. *Energies* **2020**, *13*, 3455. [CrossRef]
12. Vermeer, W.; Mouli, G.R.C.; Bauer, P. Real-Time Building Smart Charging System Based on PV Forecast and Li-ion Battery Degradation. *Energies* **2020**, *13*, 3415. [CrossRef]
13. Aljohani, T.M.; Ebrahim, A.F.; Mohammed, O.A. Hybrid Microgrid Energy Management and Control Based on Metaheuristic-Driven Vector-Decoupled Algorithm Considering Intermittent Renewable Sources and Electric Vehicles Charging Lot. *Energies* **2020**, *13*, 3423. [CrossRef]
14. Zimmerman, R.D.; Murillo-Sanchez, C.E.; Thomas, R.J. MATPOWER: Steady-State Operations, Planning, and Analysis Tools for Power Systems Research and Education. *IEEE Trans. Power Syst.* **2010**, *26*, 12–19. [CrossRef]
15. Zimmerman, R.; Murillo-Sanchez, C.E. Multi-Period SuperOPF User's Manual; 2013. Available online: https://matpower.org/docs/MATPOWER-manual-5.1.pdf (accessed on 1 July 2020).
16. Korea Power Exchange (KPX). Electric Power Statistics Information System. Available online: http://epsis.kpx.or.kr/ (accessed on 1 July 2020).
17. Jeon, W.; Mo, J.Y. The true economic value of supply-side energy storage in the smart grid environment—The case of Korea. *Energy Policy* **2018**, *121*, 101–111. [CrossRef]
18. Jeon, W.; Mo, J.Y.; Mount, T.D. Developing a Smart Grid that Customers can Afford: The Impact of Deferrable Demand. *Energy J.* **2015**, *36*. [CrossRef]
19. Sohn, S. *Current Status and Future Policy Challenges of Electric Vehicle and Charger*; Jeju Research Institute: Jeju, Korea, 2019.
20. Jeju Research Institute (JRI). *Electric Vehicle Trends and Statistics Monthly Report*; JRI: Jeju, Korea, 2018.
21. Jeju Special Self-Governing Province (Jeju). *Mid and Long-Term Comprehensive Plan for Deployment of EV and Fostering Related Industries (2018–2030)*; Jeju Special Self-Governing Province: Jeju, Korea, 2018.
22. Ministry of Environment (MOE). *A Study on the Promotion of Electric Vehicle Supply through Survey and Analysis of Actual Purchasers' Utilization*; MOE: Sejong, Korea, 2017.
23. IRENA. *Innovation Outlook EV Smart Charging for Electric Vehicles*; IRENA: Masdar City, United Arab Emirates, 2019.
24. Dubey, A.; Santoso, S.; Cloud, M.P.; Waclawiak, M. Determining Time-of-Use Schedules for Electric Vehicle Loads: A Practical Perspective. *IEEE Power Energy Technol. Syst. J.* **2015**, *2*, 12–20. [CrossRef]

25. Paran Energy. Company Data. 2019. Available online: http://www.paranenergy.com (accessed on 5 June 2020).
26. Xu, B.; Zhao, J.; Zheng, T.; Litvinov, E.; Kirschen, D.S. Factoring the Cycle Aging Cost of Batteries Participating in Electricity Markets. *IEEE Trans. Power Syst.* **2017**, *33*, 2248–2259. [CrossRef]